DALTON

The shapes of bis(cyclopentadienyl) complexes of the s-block metals*

Adam J. Bridgeman

University Chemical Laboratories, Lensfield Road, Cambridge, UK CB2 1EW

The structures and bonding of the bis(cyclopentadienyl) complexes of the alkaline-earth metals and the alkali metals have been studied using density functional calculations within the linear combination of Gaussian-type orbitals framework. The compounds $Ca(cp)_2$ and $Sr(cp)_2$ are predicted to have bent equilibrium structures in agreement with the experimentally determined shapes but in contrast to previous theoretical investigations; $Mg(cp)_2$ and the isoelectronic $[M(cp)_2]^-$ (M = Li, Na, K or Rb) ions are predicted to have coparallel, staggered rings. Analysis of the bonding shows that π-type interactions dominate for the complexes of the heavier metals of both groups as a result of the increased influence of the metal d functions. Their role is key to the driving force for the bent geometries of $Ca(cp)_2$ and $Sr(cp)_2$ just as it is for the anomalous shapes of some of the dihalide molecules. The key orbital interaction, however, is quite different.

Recent gas-phase[1] and solid-state[2] studies of the pentamethylcyclopentadienyl metallocenes of calcium, strontium and barium suggest bent structures with η^5 co-ordinated rings. The magnesium analogue[3] is thought to possess a regular ('linear') sandwich structure with coparallel rings. Molecular orbital calculations[1d,4] suggest that the equilibrium structures of all the isolated molecules have coparallel rings. The anomalous gas-phase structures are ascribed to the 'shrinkage effect' of large-amplitude vibrations and the observed solid structures to the effect of intermolecular and crystal-packing forces. The pattern of observed structures, however, is similar to that found for the alkaline-earth-metal dihalides; MgF_2 has a linear geometry whereas numerous experimental[5] and theoretical studies[6] on CaF_2, SrF_2 and BaF_2 and related molecules strongly suggest bent equilibrium shapes.

The bent shapes of molecules of the heavier alkaline earths have been explained using two models. In the polarized-ion approach[6d,e,n] the core electrons of the metal ion are distorted by the negatively charged ligands. The ligands then interact with the dipole they induce on the cation. This dipole is necessarily zero for a linear molecule and so bent molecules are favoured if the cation is polarizable. This model has been used to rationalize the structures of bent M(cp) (cp = cyclopentadienyl) molecules.[1b,7] The conclusions of orbital-based models have been detailed by DeKock *et al.*[6j] and are based on the $(n - 1)$d orbitals being more important to the bonding than the *n*p orbitals for the heavier alkaline earths. The arguments are most neatly summarized using valence-bond arguments. A metal, such as beryllium or magnesium, with *n*s and *n*p orbitals available for bonding will use sp hybrids in an MX_2 system and will thus favour a linear geometry. This is illustrated in Scheme 1(*a*). A metal with *n*s and $(n - 1)$d orbitals available will use sd hybrids and so will favour a 90 ° bond angle. This is illustrated in Scheme 1(*b*).

Blom *et al.*[1d] have reported all-electron Hartree–Fock (HF) calculations on calcocene $Ca(cp)_2$. Their results did not suggest any departure from a regular sandwich structure. The authors doubted the reliability of their calculations due to the error in the optimized Ca–C distances. Kaupp *et al.*[4] performed pseudopotential calculations at the HF, second-order Møller–Plesset perturbation (MP2) and configuration interaction single and double (CISD) levels on $M(cp)_2$ (M = Ca, Sr, Ba, Sm, Eu or Yb). Only large-scale MP2 calculations on $Ba(cp)_2$ predicted a genuinely bent equilibrium geometry. All other calculations led to regular sandwich structures. The energy required to bend the remaining systems was found to be quite small and it was concluded that this would lead to bending modes with large enough amplitudes to give the bent thermal average structures observed by the gas-phase electron diffraction studies[1]. The smaller tendency for bent structures was ascribed by these workers to the dominance of π-bonding interactions in the metallocenes compared to the predominately σ bonding found in the dihalides.

(*a*) sp hybridization

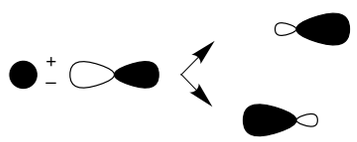

(*b*) sd hybridization

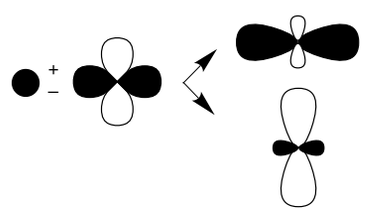

Scheme 1

The solid-state structures of $M(C_5Me_5)$ (M = Ca or Ba) reveal close packing resulting in the reasonably close approach of the face of a third C_5Me_5 ring to the metal. Williams *et al.*[2b] made a detailed comparison of the regular trends in the cp–M–cp angles (M = Ca, Ba, Eu, Sm or Yb) and concluded that the proximity of the molecules in the solid does *not* provide an adequate explanation for the observed bent geometries. The bent structures, it is concluded, must have intramolecular origins.

An alternative source of the apparently anomalous structures of these metallocenes has been suggested by Anderson *et al.*[1b] and later reintroduced and quantified by self-consistent molecular mechanics force-field calculations by Burdett and co-workers.[8] They propose that the bent shapes result from a tendency to reduce the distances between the methyl substituents on the two rings to increase the van der Waals attractions.

Density functional (DF) calculations are becoming an

* *Non-SI unit employed*: eV ≈ 1.60×10^{-19} J.

increasingly popular method of studying the properties of transition-metal compounds.[9–12] Molecular properties derived from DF calculations are often closer to experiment than those obtained from HF and post-HF studies especially for transition-metal systems. The apparently anomalous gas-phase and solid-state structures of the alkaline-earth metallocenes warrant further study. This paper reports a reinvestigation of the bonding and geometry of the metallocenes of Group 2 using local density functional (LDF) calculations in the linear combination of Gaussian-type orbitals (LCGTO) framework.

The metallocenes of the alkali metals were among the first known organometallics.[13] Very recently this area of chemistry has received new impetus through the synthesis and structural characterization of the simple metallocene sandwiches lithocene[14,15] and sodocene.[16] These $[M(cp)_2]^-$ systems possess two coparallel η^5-cp rings. The complexes are isoelectronic with the alkaline-earth-metal analogues. The LDF study has been extended to these complexes and to the, as yet, unknown 'potassocene' and 'rubidocene'; $[K(cp)_2]^-$ and $[Rb(cp)_2]^-$ respectively. The latter are isoelectronic with $Ca(cp)_2$ and $Sr(cp)_2$ and it is of interest to investigate the bonding and to predict whether these systems will be structurally different to the alkaline-earth molecules.

Computational Details

All DF calculations were performed using the 'DEFT' code written by St-Amant[17] in the LCGTO framework. Two types of calculation have been completed differing in the treatment of the exchange and correlation interactions. The first, labelled VWN, used the Vosko–Wilk–Nusair local spin density (LSD) approximation of the exchange-correlation potential.[18] The second, labelled BP, corrects the LSD expression using the Becke[19] non-local functional for exchange and the Perdew[20] non-local functional for correlation. All-electron calculations were performed on the $M(cp)_2$ (M = Mg, Ca or Sr) and $[M(cp)_2]^-$ (M = Li, Na, K or Rb) systems. Only the M–C bond lengths and the cp–M–cp bond angles were optimized. The C–C and C–H bond lengths were taken to be 1.40 and 1.06 Å respectively. To aid comparison with the results of DeKock *et al.*,[6j] the metal and the centroids of the rings were placed in the *xy* plane with the *x* axis bisecting cp–M–cp. The centroids then lie on the *y* axis in the coparallel geometry. This coordinate scheme, shown in Fig. 1, has the advantage that the d_{z^2} population should not change greatly with changes in the distortion angle. Calculations were performed with the rings eclipsed and with the rings staggered. Bending results in a reduction in symmetry from D_{5h} to C_{2v} symmetry and from D_{5d} to C_s symmetry in the eclipsed and staggered forms respectively.

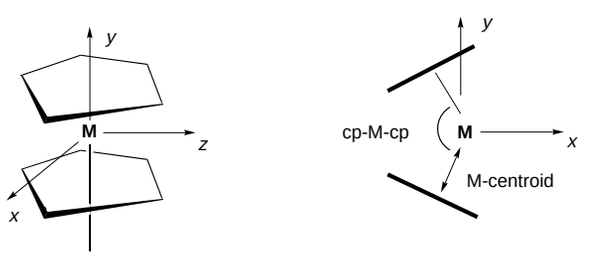

Fig. 1 Definitions of axes and structural parameters for $M(cp)_2$ systems

The Gaussian basis sets (GTOs) and the auxiliary basis sets needed for the Coulomb and exchange potential were optimized specifically for LSD calculations by Godbout *et al.*[21] The GTO sets of double-ζ quality with the contraction patterns[22] (41/1*), (721/1/1*), (721/51/41*), (6321/411/41*), (6321/411/41*), (63321/5211/1*), (63321/5211/41*), (633321/53211/51*) and (633321/53211/531*) were used for hydrogen, lithium, carbon, sodium, magnesium, potassium, calcium, rubidium and strontium respectively. Metal–carbon and carbon–carbon bond orders were calculated from the density matrix according to the prescription suggested by Mayer.[23,24] The Mulliken-population and bond-order analyses were performed using the results from the BP calculations.

Results and Discussion

Alkaline-earth metallocenes

***(a)* Geometries.** Table 1 lists the optimized geometries for the $M(cp)_2$ (M = Mg, Ca or Sr) systems together with a comparison with the experimentally determined structures. Table 2 lists the energy required to bend and dissociate the molecules. The compound $Mg(cp)_2$ is predicted to have coparallel and staggered rings in agreement with the reported crystal structure.[3] The Mg–C and magnesium–centroid distances are in good agreement with those determined experimentally.

Both $Ca(cp)_2$ and $Sr(cp)_2$ are predicted to have bent equilibrium structures with the rings staggered. The energy required to force these molecules into coparallel forms is calculated to be 10 and 12 kJ mol^{-1} respectively consistent with the bent gas-phase[1] and solid-state structures[2] and suggesting that they are genuinely bent. These results are in direct contrast to the

Table 1 Calculated and experimental geometry parameters for $M(cp)_2$ systems (M = Mg, Ca or Sr)

	$M(cp)_2$	M–C/Å	M–centroid/Å	cp–M–cp/°
Mg	X-Ray	2.339[a]	2.020	180
	VWN	2.270	1.930	180
	BP	2.360	2.040	180
Ca	Electron diffraction	2.609[b]	2.312	154
	X-Ray	2.64[c]	2.35	147.7, 146.3
	VWN	2.540	2.240	150
	BP	2.580	2.290	150
Sr	Electron diffraction	2.750[b]	2.469	149
	VWN	2.600	2.310	145
	BP	2.680	2.400	145

[a] Ref. 3. [b] Ref. 1. [c] Ref. 2.

Table 2 Dissociation and bending energies (kJ mol^{-1}) and M–C and C–C bond orders for the $M(cp)_2$ systems (M = Mg, Ca or Sr). Free $[C_5H_5]^-$ has a C–C bond order of 1.45

	Dissociation energy			Bond order			
				M–C		C–C	
Compound	Homolytic[a]	Heterolytic[b]	ΔE[c]	Coparallel	Bent	Coparallel	Bent
$Mg(cp)_2$	620	2480	−20[d]	0.26	0.21	1.33	1.36
$Ca(cp)_2$	800	2200	10	0.17	0.19	1.30	1.27
$Sr(cp)_2$	845	2120	12	0.17	0.17	1.25	1.24

[a] For process $M(cp)_2 \longrightarrow M + 2cp$. [b] For process $M(cp)_2 \longrightarrow M^{2+} + 2cp^-$. [c] For process bent form $\longrightarrow$ parallel form. [d] Taking a bent geometry of 150°.

Table 3 Mulliken metal charges q(M) and orbital populations* for the $M(cp)_2$ systems (M = Mg, Ca or Sr)

			Metal orbital populations								
Compound	cp–M–cp/°	q(M)	s	p_x	p_y	p_z	d_{xy}	d_{xz}	d_{yz}	$d_{x^2-y^2}$	d_{z^2}
$Mg(cp)_2$	180	+0.66	0.45	0.30	0.29	0.30	—	—	—	—	—
	150	+0.75	0.47	0.30	0.30	0.31					
$Ca(cp)_2$	180	+0.93	0.12	0.06	0.03	0.06	0.28	0.03	0.28	0.18	0.03
	150	+0.89	0.12	0.04	0.04	0.05	0.23	0.07	0.26	0.27	0.04
$Sr(cp)_2$	180	+0.98	0.14	0.04	0.04	0.06	0.26	0.02	0.26	0.17	0.02
	145	+0.93	0.14	0.04	0.04	0.05	0.20	0.05	0.24	0.27	0.03

* The metal and the ring centroids lie in the xy plane with the x axis bisecting cp–M–cp as shown in Fig. 1. The magnesium d orbital populations were found to be insignificant and have been ignored.

Table 4 Symmetry-allowed overlap between the metal orbitals and those of the $(cp)_2$ fragment in coparallel and bent $M(cp)_2$ systems

$(cp)_2$ orbital	D_{5h}	$D_{\infty h}$	Metal orbitals(s)	C_{2v}	Metal orbital(s)
1	a_1'	σ_g	s, $d_{x^2-y^2}$	a_1	s, p_x, $d_{x^2-y^2}$, d_{z^2}
2	a_2''	σ_u	p_y	b_1	p_y, d_{xy}
3	e_1' (i)	π_u (i)	p_x	a_1	s, p_x, $d_{x^2-y^2}$, d_{z^2}
4	e_1' (ii)	π_u (ii)	p_z	b_2	p_z, d_{xz}
5	e_1'' (i)	π_g (i)	d_{xy}	b_1	p_y, d_{xy}
6	e_1'' (ii)	π_g (ii)	d_{yz}	a_2	d_{yz}

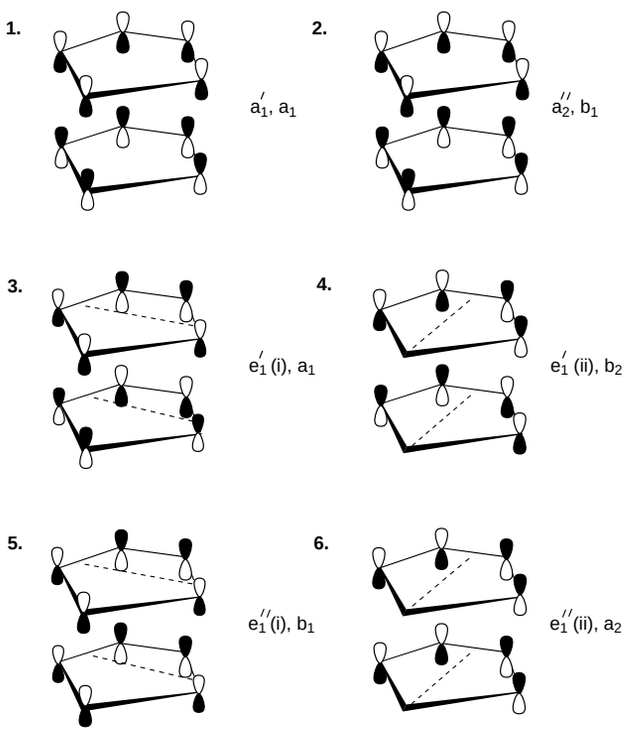

Fig. 2 Ligand π orbitals available to overlap with a metal in $M(cp)_2$ systems. The functions are labelled in D_{5h} and C_{2v} symmetry appropriate to the molecule with the rings coparallel and bent respectively

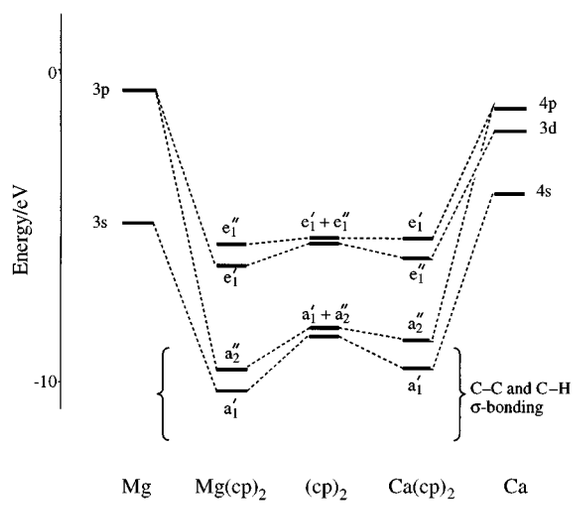

Fig. 3 Kohn–Sham eigenvalue diagram for $Mg(cp)_2$ and $Ca(cp)_2$ with the rings coparallel

previous theoretical studies by Blom *et al.*[1d] and by Kaupp *et al.*[4] The M–C and metal–centroid distances are again in reasonable agreement with the experimental values although the non-local corrections used in the BP calculations appear to be necessary to obtain accurate structures. In each case the energy difference between the conformations with the rings eclipsed and staggered was found to be 1 kJ mol^{-1}, or less. The analysis of the bonding described below was performed on the eclipsed forms to take advantage of the considerably higher (C_{2v}) symmetry.

***(b)* Bonding.** Tables 2 and 3 list the bond orders and the Mulliken metal charges and populations respectively. The bonding is shown to weaken and to become more ionic along the series Mg, Ca, Sr as expected on the basis of the metals' ionization energy and size. The orbital populations in $Ca(cp)_2$ and $Sr(cp)_2$ are quite similar although the latter is predicted to be slightly more ionic. The bond orders correlate well with the heterolytic dissociation energies listed in Table 2. The homolytic dissociation energies follow the reverse trend with $Mg(cp)_2 < Ca(cp)_2 < Sr(cp)_2$ reflecting the increasing ease of ionizing the metal. Comparison of the C–C bond order with that in the free ligand shows the effect of donation from the filled π-bonding orbitals to the metal.

The bonding in regular sandwich compounds of the transition metals has been described many times.[25] The filled ring π orbitals available for bonding to a metal are sketched in Fig. 2 and are labelled in both D_{5h} (rings coparallel and eclipsed) and in C_{2v} (rings bent and eclipsed) symmetry. The a_1' and a_2'' combinations can be thought of as 'σ_g' and 'σ_u' functions respectively to assist comparison with the dihalide systems. The e_1' and e_1'' combinations can similarly be labelled as 'π_u' and 'π_g' respectively. The metal orbitals that are able to overlap with these functions are listed in Table 4.

Fig. 3 shows the calculated Kohn–Sham eigenvalue diagrams for $Mg(cp)_2$ and $Ca(cp)_2$ with the rings eclipsed and coparallel. The most obvious difference between the two schemes is the relative energies of the e_1' and e_1'' levels. The stabilization of these orbitals is directly related to the availability of p and d functions on the metal, as shown in Table 4. As found in

Table 5 Contributions (%) to the overall M–C orbitals of the $M(cp)_2$ (M = Mg, Ca or Sr) systems by overlap of the metal valence orbitals with the ligand functions shown in Fig. 2

	$Mg(cp)_2$			$Ca(cp)_2$			$Sr(cp)_2$		
Orbital	180	150°		180	150°		180	145°	
$1\ a_1' \longrightarrow a_1$	26	26		18	16		16	15	
$2\ a_2'' \longrightarrow b_1$	17 } 43σ	14 } 40σ		9 } 27σ	10 } 26σ		7 } 23σ	9 } 24σ	
$3\ e_1'$ (i) $\longrightarrow a_1$	20	25		10	25		8	28	
$4\ e_1'$ (ii) $\longrightarrow b_2$	20	18		10	10		9	10	
$5\ e_1''$ (i) $\longrightarrow b_1$	9 } 58π	9 } 60π		27 } 74π	20 } 75π		30 } 77π	20 } 76π	
$6\ e_1''$ (ii) $\longrightarrow a_2$	9	8		27	20		30	18	

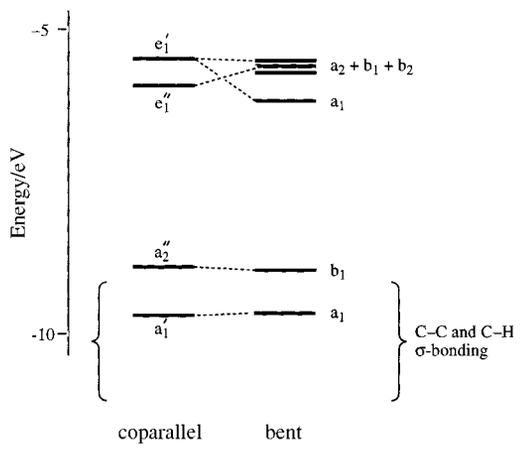

Fig. 4 Kohn–Sham eigenvalue diagram for $Ca(cp)_2$ showing the correlation between the coparallel and bent forms

previous studies of alkaline-earth-metal dihalides and related systems,[6] the most accessible valence orbitals for calcium are the 4s and 3d. The 3d orbitals of magnesium lie too far above the 3s and 3p functions to contribute significantly to the bonding. Fig. 4 shows the effect of bending the molecule on the energy levels of $Ca(cp)_2$.

Evans *et al.*[26] have reported the photoelectron (PE) spectrum of $Mg(cp)_2$. The lowest-energy pair of bands between 8 and 10 eV correspond to ionization of the highest occupied levels. The spectrum also shows a broad band between 12 and 14 eV assigned to ionization of the ring σ bonds and the remaining π levels. Ionization energies have been calculated using Slater's transition-state method.[27] The lowest ionization is predicted to occur at 6.9 eV from the e_{1g} levels (e_1'' in the staggered conformation). This corresponds to the peak at *ca.* 8.2 eV in the PE spectrum. The next ionization is predicted to occur at 8.2 eV from the e_{1u} levels (e_1' in the staggered form). This corresponds to the experimental band at *ca.* 9 eV. Ionization of the C–H and C–C bond orbitals is predicted to occur above 10.1 eV. Ionization of the remaining π levels is predicted to occur at 12.4 and 12.8 eV for the a_{1g} and a_{2u} levels (corresponding to a_1' and a_2'' in the staggered molecule) respectively. The calculations presented here are thus entirely consistent with the assignment of the PE spectrum proposed by Evans *et al.*[26]

Table 5 lists the percentage contributions to the M–C bond orders by the orbitals formed by overlap of the metal valence orbitals and the ligand functions shown in Fig. 2. The 'π' contribution only slightly exceeds the 'σ' contribution to the bond order in $Mg(cp)_2$ whilst it is dominant in $Ca(cp)_2$ and $Sr(cp)_2$. This is in direct contrast to the bonding in the dihalides where the covalent bonding[6] is predominantly due to the interaction with the σ orbitals. The importance of the 'π' bonding in $Ca(cp)_2$ and $Sr(cp)_2$ is primarily due to the greater contribution of the metal d orbitals. The bonding appears to be quite similar in these two compounds with a slightly larger contribution from the valence d orbitals in the strontium system. In view of the similarities between these two molecules, the discussion below is confined to a comparison between $Ca(cp)_2$ and $Mg(cp)_2$.

(*i*) 'σ' *Interactions.* The a_1' orbital predominantly interacts with the metal *n*s orbital. This is the most accessible metal orbital. As a result there is very little contribution from the calcium $d_{x^2-y^2}$ to this orbital in $Ca(cp)_2$. Any contribution by the $d_{x^2-y^2}$ orbital would favour a linear geometry. Upon bending this orbital is also able to interact with the metal p_x orbital. Any contribution by the p_x orbital favours a bent geometry. The strong influence of the metal s orbital results in very little contribution by the magnesium p_x orbital in the bent form of $Mg(cp)_2$.

The dominant contribution by the metal *n*s orbital to this orbital is shown by the very small changes in its energy and in its contribution to the overall metal–ring bonding upon bending in $Mg(cp)_2$ and, as shown in Fig. 4, in $Ca(cp)_2$. The non-directional nature and the increasingly diffuse nature of the *n*s orbital for the heavier metals leads to a reduction in its bonding contribution. This also results in the small population of the *n*s orbital in $Ca(cp)_2$. The a_2'' ligand combination is able to overlap with the metal p_y orbital. This is an accessible orbital for magnesium resulting in a substantial contribution to the Mg–cp bonding. The overlap is rapidly lost upon bending and this is reflected in the reduction in the contribution to the bond order shown in Table 5. The molecular function rises in energy by ≈ 0.1 eV when the molecule is bent by 30 °. The contribution is much less important for $Ca(cp)_2$ due to the lesser influence of the metal p functions in the bonding. This ligand combination can overlap with the d_{xy} in the bent form. The analogous interaction has been shown to be the main orbital factor favouring bent geometries in the alkaline-earth-metal dihalides.[6] For $Ca(cp)_2$, as shown in Table 5 and Fig. 4, there is only a very small increase in the bonding due to this overlap when the molecule is bent. This is consistent with the much lower influence of σ-type bonding in the metallocene. In addition, this ligand combination leads to an antibonding interaction between the rings themselves. This is insignificant in the coparallel form but begins to destabilize the molecule as the large ligands are brought closer together upon bending.

(*ii*) 'π' *Interactions.* The ligand e_1' combinations are able to overlap with the metal p_x and p_z functions but the interaction is relatively poor because of the 'side-on' nature of the overlap. This leads to the lesser importance of π-type bonding in $Mg(cp)_2$. The overlap of the a_1 function [(i) of the e_1' pair] with the metal p_x orbital improves and becomes more 'σ' in appearance when the rings are moved towards the *x* axis as the molecule is bent. This is pictured in Fig. 5(*a*). It results in a substantial increase in the bonding contribution from this overlap and a stabilization of the molecular function by ≈0.5 eV upon bending for $Mg(cp)_2$. The overlap of the second member of the e_1' pair with the metal p_z orbital changes little as the molecule is bent. The energy and bonding contribution from the resulting molecular function does not vary greatly with the cp–Mg–cp angle.

The relatively high energy of the calcium p orbitals results in small p_x and p_z populations and weak bonding from overlap

with the ligand e_1' combination in coparallel $Ca(cp)_2$. Upon bending, the a_1 ligand function [(i) of the e_1' pair] is able to overlap with the metal $d_{x^2-y^2}$ orbital. This is pictured in Fig. 5(*b*). It results in a large increase in the $d_{x^2-y^2}$ population and in the bonding contribution from the molecular function. The eigenvalue decreases by ≈0.75 eV. It then lies lower than the functions derived from the ligand e_1'' combinations in the bent form, as shown in Fig. 4. This appears to be the dominant orbital factor in the observed bent geometries of $Ca(cp)_2$ and $Sr(cp)_2$.

The second member of the e_1' pair is able to overlap with the metal d_{xz} orbital when the molecule is bent. This makes a much smaller contribution to the stabilization of the bent form.

The ligand e_1'' combinations are able to overlap well with metal d_{xy} and d_{yz} orbitals and this is responsible for the large π-type bonding in coparallel $Ca(cp)_2$. The overlap decreases upon bending resulting in a reduction in the contribution to the bonding. This factor is the major orbital influence favouring a coparallel geometry for the calcium and strontium systems. It is insufficient to compensate for the enhanced bonding of the a_1 function shown in Fig. 5(*b*).

Alkali-metal metallocenes

Table 6 lists the optimized geometries for the $[M(cp)_2]^-$ (M = Li, Na, K or Rb) systems together with a comparison with the experimentally determined structures of $[Li(cp)_2]^-$ and $[Na(cp)_2]^-$. All the ions are predicted to have staggered and coparallel rings. This agrees with the known structures[14–16] of lithocene and sodocene. The calculated dissociation and bending energies and M–C and C–C bond orders are listed in Table 7. The ions $[K(cp)_2]^-$ and $[Rb(cp)_2]^-$ are isoelectronic with $Ca(cp)_2$ and $Sr(cp)_2$. Whilst the latter pair are predicted to have bent equilibrium structures in agreement with diffraction studies,[1,2] the alkali-metal analogues are predicted to have coparallel rings. The energy required to bend these molecules is predicted to be rather small. Packing and intermolecular forces in the solid state could well influence the geometries that would be adopted by these, as yet unknown, systems.

The bond lengths and orders and the dissociation energies indicate, as expected, rather weaker bonding than in the alkaline-earth-metal molecules. Although the dissociation energies decrease as Group 1 is descended and the M–C bond order is largest for M = Li, it is approximately equal for M = Na, K or Rb. The metal charges suggest that, as expected, lithocene is the most covalently bonded system but that $[K(cp)_2]^-$ and $[Rb(cp)_2]^-$ are less ionic than sodocene. The Mulliken orbital populations (Table 8) show that the source of the lower metal charges for M = K and Rb is the large d orbital populations. Table 9 breaks down the M–C bond order into the contributions from molecular functions formed by overlap of the metal orbitals with the ligand combinations pictured in Fig. 2. The influence of the d orbitals of K and Rb is shown by the greater contribution of π-type bonding in $[K(cp)_2]^-$ and $[Rb(cp)_2]^-$. A similar result was noted for the alkaline-earth-metal analogues. Potassium and rubidium utilize s, p and d orbitals in these quite covalently bonded molecules. The s and d functions appear to be the most important for these pre-transition elements.

The changes in overlap and orbital energies with the cp–M–cp angle follow a similar pattern to those described above for the alkaline earths. The increased overlap with the a_1 ligand function [(i) of the e_1' pair] upon bending was described above as the driving force for the observed bent geometries of $Ca(cp)_2$ and $Sr(cp)_2$. Only a small stabilization in the analogous molecular function was found for the isoelectronic alkali-metal systems. This is a reflection of the overall weaker and more ionic bonding in these systems. The stabilization is insufficient to favour bent molecules.

Conclusion

The DF calculations on the bis(cyclopentadienyl) complexes of the alkaline-earth metals predict coparallel structure for $Mg(cp)_2$ but bent geometries for $Ca(cp)_2$ and $Sr(cp)_2$. The calculated structures are in good agreement with those determined by electron[1] and X-ray[2,3] diffraction. The results contrast with

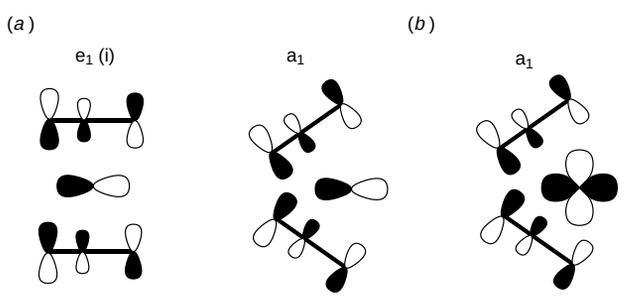

Fig. 5 Key orbital interaction favouring a bent geometry in $M(cp)_2$ systems with (*a*) a metal utilizing p orbitals and (*b*) a metal utilizing d orbitals

Table 6 Optimized geometries for the $[M(cp)_2]^-$ (M = Li, Na, K or Rb) systems together with a comparison with the experimentally determined structures of $[Li(cp)_2]^-$ and $[Na(cp)_2]^-$; cp–M–cp 180° in each case

$[M(cp)_2]^-$		M–C/Å	M–centroid/Å
Li	X-Ray[a]	2.318	2.008
	VWN	2.200	2.033
	BP	2.290	2.130
Na	X-Ray[b]	2.630	2.346
	VWN	2.600	2.461
	BP	2.700	2.566
K	VWN	2.800	2.671
	BP	2.820	2.692
Rb	VWN	2.970	2.850
	BP	3.020	2.901

[a] Refs. 14 and 15. [b] Ref. 16.

Table 7 Dissociation and bending energies (kJ mol^{-1}) and M–C and C–C bond orders for the $[M(cp)_2]^-$ systems (M = Li, Na, K or Rb). Free $[C_5H_5]^-$ has a C–C bond order of 1.45

			Bond order			
			M–C		C–C	
Compound	Dissociation energy[a]	ΔE[b]	Coparallel	Bent[c]	Coparallel	Bent[c]
$[Li(cp)_2]^-$	925	−30	0.15	0.12	1.39	1.42
$[Na(cp)_2]^-$	751	−18	0.10	0.08	1.41	1.42
$[K(cp)_2]^-$	733	−5	0.11	0.10	1.41	1.41
$[Rb(cp)_2]^-$	720	−5	0.10	0.10	1.41	1.40

[a] For process $[M(cp)_2]^- \longrightarrow M^{2+} + 2cp^-$. [b] For process bent form ⟶ parallel form. [c] Taking a bent geometry of 150°.

Table 8 Mulliken metal charges q(M) and orbital populations[a] for the $[M(cp)_2]^-$ systems (M = Li, Na, K or Rb)

		Metal orbital population					
Compound	q(M)	s	$p_{x,z}$	p_y	$d_{xy,yz}$	d_{xz,z^2}	$d_{x^2-y^2}$
$[Li(cp)_2]^-$	+0.27	0.20	0.17	0.19		*b*	
$[Na(cp)_2]^-$	+0.50	0.18	0.11	0.10		*b*	
$[K(cp)_2]^-$	+0.40	0.11	0.05	0.04	0.13	0.00	0.08
$[Rb(cp)_2]^-$	+0.41	0.08	0.07	0.05	0.12	0.01	0.06

[a] The C_5 axis is taken parallel to the y axis. [b] d Orbital populations found to be insignificant.

Table 9 Contributions (%) to the overall M–C orbitals of the $[M(cp)_2]^-$ (M = Li, Na, K or Rb) systems by overlap of the metal valence orbitals with the ligand functions shown in Fig. 2

Orbital	$[Li(cp)_2]^-$	$[Na(cp)_2]^-$	$[K(cp)_2]^-$	$[Rb(cp)_2]^-$
$1\ a_1'$	21 } 40σ	33 } 50σ	18 } 31σ	21 } 24σ
$2\ a_2''$	19 }	17 }	13 }	13 }
$3/4\ e_1'$	50 } 60π	44 } 50π	25 } 69π	20 } 65π
$5/6\ e_1''$	10 }	6 }	44 }	45 }

those reported for molecular orbital calculations.[1d,4] These calculations predicted coparallel geometries for all of these molecules. It was suggested[4] that the observed gas-phase structures were a result of the 'shrinkage effect' of high-amplitude bending motions and that the bent solid-state structures were determined by intermolecular interactions. The DF calculations predict that the equilibrium structures are *genuinely* bent.

Dissection of the bonding characteristics provided by analysis of the density matrix suggests that the calcium and strontium s and d functions are important in the covalent interactions. The contribution of the metal d orbitals leads to dominant π-type bonding. This contrasts with the much greater importance of σ interactions in $Mg(cp)_2$. The π-type bonding is, however, more important in all of these metallocenes than for the dihalides and related systems.[6]

The driving force for the bent structures of $Ca(cp)_2$ and $Sr(cp)_2$ appears to be the increased overlap and interaction of the metal $d_{x^2-y^2}$ orbital with the a_1 ligand function [(i) of the e_1' pair] pictured in Fig. 5(*b*). This should be compared with the suggestion[6] that the bent dihalides of the heavier alkaline earths result from the increased overlap with the halide σ_u combination upon bending. Quite different ligand functions are involved in these key orbital interactions in the $M(cp)_2$ and dihalide molecules. The bent geometries result in both cases, however, from overlap of ligand orbitals with low-lying d functions on the metal.

As discussed briefly above, the origin of the anomalous, bent structures of the $M(cp)_2$ (M = Ca, Sr, Ba, Sm, Eu or Yb) was suggested by Anderson *et al.*[1b] and later by Burdett and coworkers[8] to be due to van der Waals interactions between the ligands. The cp ligands are negatively charged in these reasonably ionic systems and are relatively bulky so that close approach would not seem to be favourable. If an attractive force between the ligands were actually dominant in these systems then presumably it would be a common feature in the structural chemistry of sandwich complexes. It is not.

The $M(cp)_2$ complexes of the transition metals appear to have regular structures[28] with coparallel rings except where distortion occurs because of dimerization. There is clearly an electronic influence favouring coplanar rings due to the presence of d electrons in these systems. The $M(cp)_2$ complexes of the Group 14 elements appear to have genuinely bent structures[29] in the gas phase unless there are bulky substituents on the rings. The structural similarities between the Group 2 and Group 14 systems has been noted[8,30] and it was suggested that the van der Waals model be applied to both sets. The more usual interpretation of the bent shapes of the $M(cp)_2$ molecules of the Group 14 elements is the stereochemical presence of a lone pair on the metal. The presence of this lone pair may also be inferred from the structure[31] of the orthorhombic polymorph of $Pb(cp)_2$. This contains chains of {–cp–Pb–cp–} units with the lone pair on each Pb presumably being used to bond to a neighbouring ring in the chain.

The most compelling chemical evidence for the direct electronic influence of the metal in determining the bent shapes of the $M(cp)_2$ molecules of the Group 2 and 14 elements comes from a comparison with the structures of related systems. The dihalides of magnesium and the 3d transition metals appear to be linear[5] and their $M(cp)_2$ complexes have coparallel rings.[28] The compounds CaF_2, SrF_2, BaF_2 and $YbCl_2$ appear[5,32] to be bent as do $Ca(cp)_2$, $Sr(cp)_2$ and $Yb(cp)_2$. The stereochemical activity of the lone pair of electrons on the Group 14 metals is clear in the structural chemistry of the divalent elements.[33] The shapes of the Group 14 bis(cyclopentadienyl) systems do not appear to be exceptional.

As detailed above, the anomalous shapes of $Ca(cp)_2$ and $Sr(cp)_2$ and of other MX_2 systems[6j] appear to be due to the influence of the low-lying d orbitals although the roles appear to be somewhat different in the two sets. This is not to say that the electronic interactions between the cp rings are unimportant. The all-electron calculations described in this paper seek to include all such effects. The key orbital overlap in $Ca(cp)_2$ favouring a bent geometry leads to a bonding interaction between the rings and this helps to ensure that sizeable angular distortion results.

The DF calculations on the $[M(cp)_2]^-$ sandwich complexes of the alkali metals predict coparallel rings in each. The bonding appears to be very similar to that in the alkaline-earth-metal systems although it is, as expected, somewhat weaker. Although $[K(cp)_2]^-$ and $[Rb(cp)_2]^-$ are predicted to have coparallel rings, the energy required to bend the molecules appears to be rather small. The increased overlap of the metal $d_{x^2-y^2}$ with the a_1 ligand function again provides a driving force for bending but the interaction is too small to result in a genuinely bent equilibrium geometry. It should be noted that any attractive interaction between the ligands is insufficient to produce bent shapes. These ions are, as yet, unknown but should be at least as stable as the structurally characterized sodocene anion. The low bending energy could well result in intermolecular forces having a large influence on the structure of these ions.

Acknowledgements

The author would like to thank Dr Alain St-Amant of the University of Ottawa for making the DEFT code publicly available.

References

1 (*a*) R. A. Anderson, J. M. Boncella, C. J. Burns, R. Blom, A. Haaland and H. V. Volden, *J. Organomet. Chem.*, 1986, **312**, C49; (*b*) R. A. Anderson, R. Blom, J. M. Boncella, C. J. Burns and H. V. Volden, *Acta Chem. Scand., Ser. A*, 1987, **41**, 24; (*c*) R. A. Anderson, R. Blom, J. M. Boncella, C. J. Burns and H. V. Volden, *J. Chem. Soc. Chem. Commun.*, 1987, 768; (*d*) R. Blom, K. Faegri, jun. and H. V. Volden, *Organometallics*, 1990, **9**, 372.

2 R. A. Williams, T. P. Hanusa and J. C. Huffman, (*a*) *J. Chem. Soc., Chem. Commun.*, 1988, 1045; (*b*) *Organometallics*, 1990, **9**, 1128.
3 W. Bunder and E. Weiss, *J. Organomet. Chem.*, 1975, **92**, 1.
4 M. Kaupp, P. v. R. Schleyer, M. Dolg and H. Stoll, *J. Am. Chem. Soc.*, 1992, **114**, 8202.
5 M. Hargittai, *Coord. Chem. Rev.*, 1988, **91**, 35 and refs. therein.
6 (*a*) E. F. Hayes, *J. Phys. Chem.*, 1966, **70**, 3740; (*b*) D. R. Yarkonyi, W. J. Hunt and H. F. Schäffer, *Mol. Phys.*, 1973, **26**, 941; (*c*) J. L. Gole, A. K. Q. Siu and E. F. Hayes, *J. Chem. Phys.*, 1973, **58**, 857; (*d*) M. Guido and G. Gigli, *J. Chem. Phys.*, 1974, **61**, 4138; (*e*) M. Guido and G. Gigli, *J. Chem. Phys.*, 1976, **65**, 1397; (*f*) D. M. Hassett and C. J. Marsden, *J. Chem. Soc. Chem. Commun.*, 1990, 667; (*g*) J. M. Dyke and T. G. Wright, *Chem. Phys. Lett.*, 1990, **169**, 138; (*h*) L. v. Szentpály and P. Schwerdtfeger, *Chem. Phys. Lett.*, 1990, **170**, 555; (*i*) U. Salzner and P. v. R. Schleyer, *Chem. Phys. Lett.*, 1990, **172**, 461; (*j*) R. L. DeKock, M. A. Peterson, L. K. Timmer, E. J. Baerends and P. Vernooijs, *Polyhedron*, 1990, **9**, 1919; (*k*) M. Kaupp and P. v. R. Schleyer, *J. Chem. Phys.*, 1991, **94**, 1360; (*l*) L. Seijo, Z. Barandiarán and S. Huzinaga, *J. Chem. Phys.*, 1991, **94**, 3762; (*m*) M. Kaupp and P. v. R. Schleyer, *J. Am. Chem. Soc.*, 1992, **114**, 491; (*n*) I. Bytheway, R. J. Gillespie, T.-H. Tang and R. F. W. Bader, *Inorg. Chem.*, 1995, **34**, 2407.
7 W. J. Evans, L. S. Hughes and T. P. Hanusa, *Organometallics*, 1986, **5**, 1285.
8 J. K. Burdett, in *Accurate Molecular Structures: Their Determination and Importance*, eds. A. Domenicano and I. Hargittai, Oxford University Press, Oxford, 1992; T. K. Hollis, J .K. Burdett and B. Bosnich, *Organometallics*, 1993, **12**, 3385.
9 *Local Density Approximations in Quantum Chemistry and Solid-State Physics*, eds. J. P. Dahl and J. Avery, Plenum, New York, 1989.
10 R. G. Parr and W. Yang, *Density-Functional Theory of Atoms and Molecules*, Oxford University Press, Oxford, 1989.
11 *Density Functional Methods in Chemistry*, eds. J. K. Labanowski and J. W. Andelm, Springer, New York, 1991.
12 T. Ziegler, *Chem. Rev.*, 1991, **91**, 651.
13 J. Thiele, *Dtsch. Chem. Ges.*, 1901, **34**, 68.
14 S. Harder and M. H. Prosenc, *Angew. Chem., Int. Ed. Engl.*, 1994, **33**, 1744.
15 D. Stalke, *Angew. Chem., Int. Ed. Engl.*, 1994, **33**, 2168.
16 S. Harder, M. H. Prosenc and U. Rief, *Organometallics*, 1996, **15**, 118.
17 A. St-Amant, DEFT, a FORTRAN program, University of Ottawa, 1994.
18 S. H. Vosko, L. Wilk and M. Nusair, *Can. J. Phys.*, 1980, **58**, 1200.
19 A. D. Becke, *Phys. Rev. A*, 1988, **38**, 3098.
20 J. P. Perdew, *Phys. Rev. B*, 1986, **33**, 8822.
21 N. Godbout, D. R. Salahub, J. Andzelm and E. Wimmer, *Can. J. Chem.*, 1992, **70**, 1992.
22 *Gaussian Basis Sets for Molecular Calculations*, ed. S. Huzinaga, Elsevier, New York, 1984.
23 I. Mayer, *Chem. Phys. Lett.*, 1983, **97**, 270.
24 I. Mayer, *Int. J. Quantum Chem.*, 1984, **26**, 151.
25 F. A. Cotton, *Chemical Applications of Group Theory*, Wiley-Interscience, New York, 1990.
26 S. Evans, M. L. H. Green, B. Jewitt, A. F. Orchard and C. F. Pygall, *J. Chem. Soc., Faraday Trans. 2*, 1972, 1847.
27 J. S. Slater, *The Calculation of Molecular Orbitals*, Wiley-Interscience, New York, 1979.
28 *Comprehensive Organometallic Chemistry*, ed. G. Wilkinson, Pergamon, New York, 1982.
29 P. Jutzi, F. Kohl, P. Hoffman, C. Krüger and Y.-H. Tsay, *Chem. Ber.*, 1980, **113**, 757; J. L. Atwood, W. E. Hunter, A. H. Cowley, R. A. Jones and C. A. Stewart, *J. Chem. Soc. Chem. Commun.*, 1981, 925; M. Grenz, E. Hahn, W.-W. du Mont and J. Pickardt, *Angew. Chem., Int. Ed. Engl.*, 1984, **23**, 61; P. Jutzi, D. Kanne and C. Krüger, *Angew. Chem., Int. Ed. Engl.*, 1986, **25**, 164.
30 D. J. Burkey and T. P. Hanusa, *Comments Inorg. Chem.*, 1995, **17**, 41.
31 C. Panattoni, G. Bombieri and U. Croato, *Acta. Crystallogr.*, 1966, **21**, 823.
32 I. R. Beattie, J. S. Ogden and R. S. Wyatt, *J. Chem. Soc., Dalton Trans.*, 1983, 2343.
33 N. N. Greenwood and A. Earnshaw, *Chemistry of the Elements*, Pergamon, Oxford, 1986.

Received 9*th May* 1997; *Paper* 7/03199H